Gene 572 (2015) 266–273

Contents lists available at ScienceDirect

Gene

journal homepage: www.elsevier.com/locate/gene

Research Paper

SNORD116 and SNORD115 change expression of multiple genes and modify each other's activity

Marina Falaleeva [b], Justin Surface [b], Manli Shen [b], Pierre de la Grange [a], Stefan Stamm [b,*]

[a] Genosplice, ICM, Pitie Salpêtrière Hospital, 75013 Paris, France
[b] Department of Molecular and Cellular Biochemistry, University of Kentucky, College of Medicine, Lexington, KY 40536, United States

ARTICLE INFO

Article history:
Received 4 May 2015
Received in revised form 23 June 2015
Accepted 8 July 2015
Available online 26 July 2015

Keywords:
snoRNA
Prader–Willi syndrome
Array analysis

ABSTRACT

The loss of two gene clusters encoding small nucleolar RNAs, *SNORD115* and *SNORD116* contribute to Prader–Willi syndrome (PWS), the most common syndromic form of obesity in humans. *SNORD115* and *SNORD116* are considered to be orphan C/D box snoRNAs (SNORDs) as they do not target rRNAs or snRNAs. *SNORD115* exhibits sequence complementarity towards the *serotonin receptor 2C*, but *SNORD116* shows no extended complementarities to known RNAs. To identify molecular targets, we performed genome-wide array analysis after overexpressing *SNORD115* and *SNORD116* in HEK 293T cells, either alone or together. We found that *SNORD116* changes the expression of over 200 genes. *SNORD116* mainly changed mRNA expression levels. Surprisingly, we found that *SNORD115* changes *SNORD116's* influence on gene expression. In similar experiments, we compared gene expression in post-mortem hypothalamus between individuals with PWS and aged-matched controls. The synopsis of these experiments resulted in 23 genes whose expression levels were influenced by *SNORD116*. Together our results indicate that *SNORD115* and *SNORD116* influence expression levels of multiple genes and modify each other activity.

1. Introduction

Prader–Willi syndrome (PWS) is a frequent genetic form of obesity in humans, characterized by hyperphagia, short stature, hypogonadism, thick saliva, obsessive–compulsive behavior, and hormonal imbalances (Butler et al., 2006; Cassidy et al., 2012). PWS patients typically undergo several stages of disease: severe infantile hypotonia with poor suck and failure to thrive after birth, followed by early-childhood onset obesity and hyperphagia. In addition, there are developmental delays and/or mild intellectual disability (Butler, 2011; Cassidy et al., 2012).

PWS is caused by the loss of gene expression from a maternally imprinted region on chromosome 15 (15q11.2–q13) that contains several protein coding genes, as well as clusters of C/D box snoRNAs (SNORDs). The two SNORD clusters encode *SNORD115* and *SNORD116*. Each cluster contains 47 and 28 similar copies, respectively. Recently, several patients with Prader–Willi like phenotype were described to have microdeletions affecting the *SNORD115* and *SNORD116* clusters (Fig. 1A). All microdeletions encompass the *SNORD116* cluster, suggesting a central role of these SNORDs. Although these patients share nutritional features, hypogonadism, behavioral problems and intellectual disability with PWS patients, the patients with microdeletions have a tall stature as children, a large head circumference and hand features atypical for PWS, suggesting that genes other than *SNORD116* contribute to PWS (Sahoo et al., 2008; de Smith et al., 2009; Duker et al., 2010; Bieth et al., 2015).

Small nucleolar RNAs (snoRNAs) are 60–300 nt long non-coding RNAs that accumulate in the nucleolus. Based on characteristic sequence elements, snoRNAs are classified as C/D box and H/ACA box snoRNAs. In humans, C/D box snoRNAs (SNORDs) are mostly derived from intronic regions, located 70–90 nt upstream of the 3′ splice site of an exon in a hosting gene (Fig. 1B). After the splicing reaction, introns are excised as lariats that are opened and subsequently degraded. snoRNAs escape this degradation by forming a protein complex (Hirose and Steitz, 2001).

Canonical C/D box snoRNAs (SNORDs) form a protein complex that includes *NOP56, NOP58* and *NHP2L1*, as well as *fibrillarin* acting as the RNA methyltransferase. RNA secondary structures formed by C (RUGAUGA, R = purine) and D (CUGA) boxes help the assembly of proteins to form a snoRNA–protein complex (snoRNP). This snoRNP exposes an RNA element, the antisense box that hybridizes to the target RNA. In the target RNA, a distinct ribose residue is 2′-O-methylated by the RNA methyltransferase *fibrillarin* (reviewed in (Smith and Steitz, 1997; Kiss, 2002; Matera et al., 2007; Reichow et al., 2007; Brown et al., 2008) and available in the LBME snoRNA database (Lestrade and Weber, 2006)).

Abbreviations: snoRNA, small nucleolar RNA; SNORD, C/D box snoRNA; PWS, Prader–Willi syndrome; RPA, RNase protection assay.

* Corresponding author at: Department of Molecular and Cellular Biochemistry, University of Kentucky, College of Medicine, 741 South Limestone, Lexington, KY 40536, United States.
E-mail address: stefan@stamms-lab.net (S. Stamm).

http://dx.doi.org/10.1016/j.gene.2015.07.023
0378-1119/

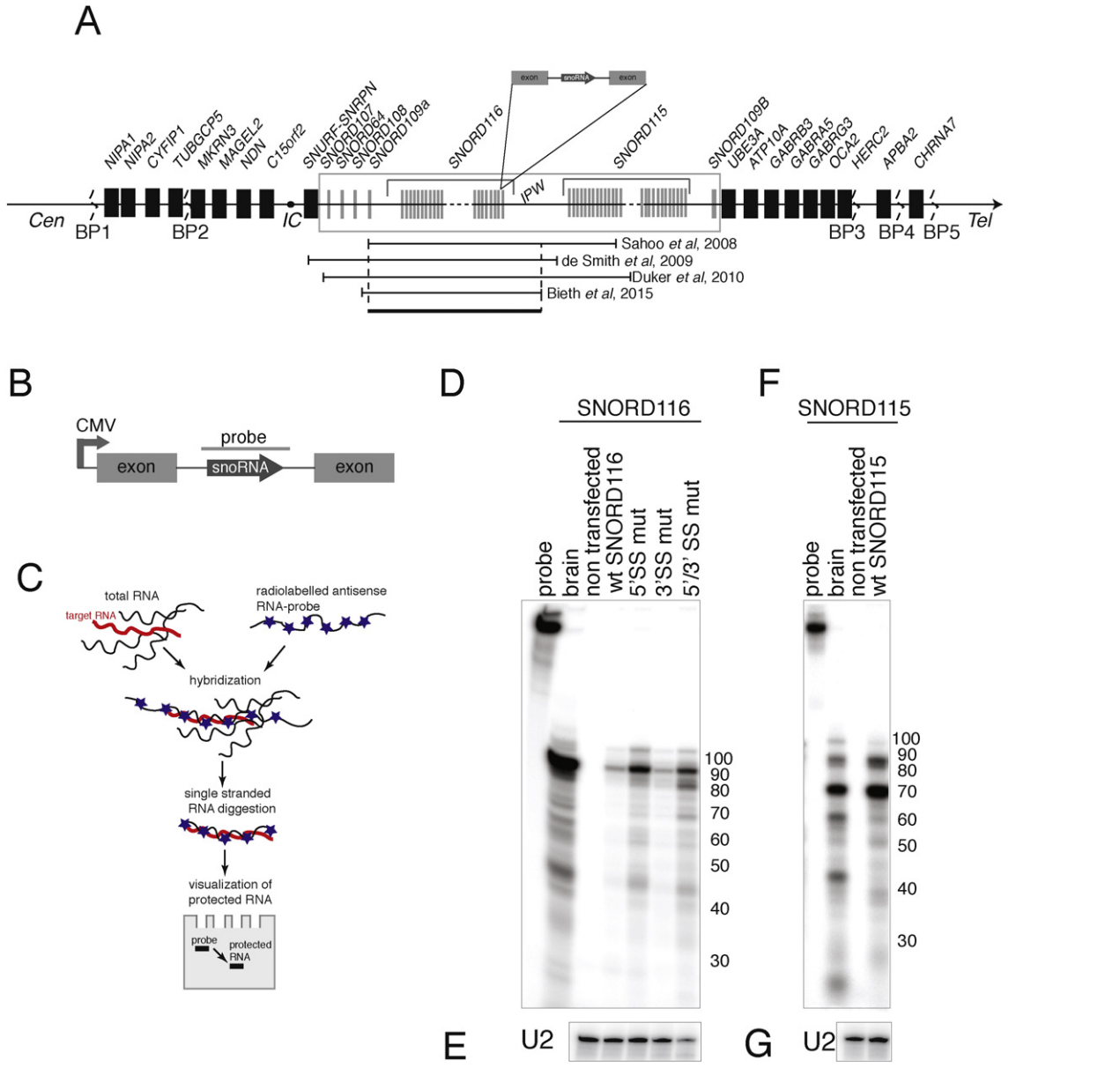

Fig. 1. Validation of SNORD expression constructs. A. Summary of the Prader–Willi critical region 15q11.2–q13. The most common break points are indicated (BP1–BP5). Protein coding genes are indicated as boxes. C/D box snoRNA expression units are indicated as gray vertical lines. Each SNORD expression unit consists of two non-coding exons flanking the intron hosting the snoRNA (schematically indicated). The SNORD116 cluster consists of 24 expression units and the SNORD115 cluster of 47 expression units. IPW: imprinted in Prader–Willi. Microdeletion of snoRNA-expressing units that cause PWS are indicated by bars. B. Schematic representation of the expression construct. C. Overview of the RNase protection assay (RPA). Total RNA is mixed with a uniformly radio-labeled antisense RNA, resulting in the hybridization between target and probe. After digestion of single stranded RNA, the protected RNAs are separated on an acrylamide gel and visualized by autoradiography. D. RNase protection assay showing SNORD116 expression derived from cDNA constructs. Mouse brain is used as a control. Non-transfected depict non-transfected HEK 293T cells, wt: cells transfected with the wild-type SNORD116 construct; 5′ SSmut: cells transfected with a SNORD construct showing a consensus 5′ splice site; 3′ SSmut: cells transfected with a snoRNA construct showing a consensus 3′ splice site; 5′/3′ SS mut: cells transfected with a construct containing both 5′ and 3′ splice sites brought into consensus. For each experiment one million cells were transfected with 1 μg of expression construct. E. RNase protection assay of U2 snRNA was used as a loading control (188 nt). F. RNase protection assay showing SNORD115 expression derived from cDNA constructs. Mouse brain is used as a control. Non-transfected depicts non-transfected HEK 293T cells, wt: cells transfected with the wild-type SNORD115 construct (Kishore and Stamm, 2006). G. RNase protection assay of U2 snRNA was used as a loading control (188 nt).

However, about half of the 267 human C/D box snoRNAs including *SNORD115* and *SNORD116* clusters show no sequence complementarity towards other ncRNAs and are thus orphan, suggesting additional functions. *SNORD115* shows an 18 nt sequence complementarity towards the *serotonin receptor 2C* and more limited complementarities to several other pre-mRNAs and changes alternative splicing in these genes (Kishore and Stamm, 2006; Kishore et al., 2010). In addition, RNase protection experiments show that both *SNORD115* and *SNORD116* form shorter RNA fragments and bind non-canonical proteins involved in RNA metabolism, such as hnRNPs (Kishore et al., 2010; Soeno et al., 2010). However, immunoprecipitates of *fibrillarin* contain *SNORD116* and *SNORD115*, suggesting that a fraction of SNORDs forms canonical snoRNA complexes (Soeno et al., 2010; Bortolin-Cavaille and Cavaille, 2012). *SNORD115* and *SNORD116* are highly conserved in vertebrate species, whereas their flanking introns and hosting exons are poorly conserved (Kishore and Stamm, 2006). This indicates that they exhibit sequence-specific functions, but until now no target genes were discovered for *SNORD116*. Recently, deep-sequencing experiments showed that other SNORDs give rise to shorter fragments (Deschamps-Francoeur et al., 2014; Dupuis-Sandoval et al., 2015). Functionally, these orphan snoRNAs have been implicated in formation of miRNAs, regulation of

chromatin structure, alternative splicing and modulation of cell survival under oxidative stress (reviewed in (Falaleeva and Stamm, 2013; Dupuis-Sandoval et al., 2015)), which increases the variety of the biological functions of SNORDs.

Here we perform genome-wide array analysis to identify genes regulated by *SNORD115/116*. The analysis indicated that *SNORD116* changes expression levels of over 200 genes. Unexpectedly, we found that *SNORD115* influences the ability of *SNORD116* to change target gene expression.

2. Material and methods

2.1. Construction of SNORD116 expression clones

For *SNORD116* overexpression, we used the mouse copy orthologous to human SNORD116-1. We previously used mouse orthologs (MBII-52 and MBII-85) of *SNORD115* and *SNORD116*, respectively as they are highly similar to the human SNORDs. Furthermore, *SNORD115* was shown to regulate human genes (Kishore and Stamm, 2006; Kishore et al., 2010). MBII-85 is >88% identical to its human counterparts. Considering G:U base-pairs forming in RNA, MBII-85 has 94% identical binding capacity compared with human. The MBII-52 sequence is >93% identical to it's human counterpart and has >96% identical binding properties. The mouse RNA is more similar to the particular human copy than some of the related human copies to each other.

The initial *SNORD116* expression cassette that represents two exons with snoRNA embedded within the intron was synthetized by Biomatik, Wilmington, USA. The constructs contain the 380 nt or 2536 nt long natural intron for *SNORD115* or *SNORD116*, respectively. To improve *SNORD116* expression efficiency site directed mutagenesis was performed using PCR primers (R-MBII-85 5′-SS: TGCAGCAATTCCCATATA ACTTACCTTTTAACTCAGGTGAC, F-MBII-85 5′-SS:GTCACCTGAGTTAAAA GGTAAGTTATATGGGAATTGCTGCA) to mutate 5′ splice site and PCR primers (R-MBII-85 3′-SS: GCAACCCTGTGAAGAGAAAAGAGAGAACA TGCCCC, F-MBII-85 3′-SS: GGGGCATGTTCTCTCTTTTCTCTTCACAGGG TTGC) to mutate 3′ splice site. All constructs are available through Addgene (ID numbers 67631, 67643–67647).

2.2. Array analysis

The transfection of cells was performed for 40 h using 2 μg of plasmid DNA for about 2×10^5 cells in six-well plate using calcium phosphate transfection method (Stoss et al., 1999).

RNA was isolated from HEK 293T cells using Total RNA RNeasy kit (Qiagen) and from brain section using RNeasy Lipid Tissue kit (Qiagen). Its quality was determined with a Bioanalyzer instrument (Agilent Technology). RNA characterized by RIN > 9.5 for HEK 293T RNA and RIN > 6 for brain section RNA were used following the Affymetrix labeling procedure.

For the analysis, the signal from Affymetrix human junction arrays (HJAY) was normalized using the "Probe scaling" method. The background was corrected with ProbeEffect from GeneBase (Kapur et al., 2008). The gene expression index was computed from probes that were selected using ProbeSelect from GeneBase (Kapur et al., 2008). The gene expression signals were computed using these probes. Genes were considered expressed if the mean intensity was ≥500. Genes were considered regulated if 1) they were expressed in at least one condition; 2) the fold-change was greater or equal than 1.5 and; 3) the unpaired t-test p-value between gene intensities was ≤0.05. For each probe, a splicing-index was computed. Unpaired t-tests were performed to determine the difference in probe expression between the two samples as described previously (Shen et al., 2010). Probe p-values in each probe set were then summarized using Fisher's method. Using annotation files, splicing patterns (cassette exons, 5′- and 3′ alternative splice sites and mutually exclusive exons) were tested for a difference between isoforms, selecting the ones with a minimum number of regulated probe sets (with a p-value ≤ 0.01) in each competing isoform (at least one third of "exclusion" probe sets have to be significant; at least one third of "inclusion" probe sets have to be significant and show an opposite regulation for the splicing-index compared with the "exclusion" probe sets). For example, for a single cassette exon, the exclusion junction and at least one of the three inclusion probe sets (one exon probe set and two inclusion junction probe sets) have to be significant and have to show an opposite regulation for the splicing-index.

2.3. RNase protection analysis (RPA)

HEK 293T cells were transiently transfected with plasmids coding for *MBII-52* and *MBII-85* snoRNA (mouse orthologous of *SNORD115-15* and *SNORD116-1* respectively). Total RNA was isolated from cells using TRIzol LS reagent according to manufacturer's protocol.

As a probe, we used a uniformly labeled RNA against mouse chr7:59,520,283-59,520,365 for MBII-52 and chr7:59,861,729-59,861,827 for MBII-85, as previously described (Shen et al., 2011).

2.4. RT-PCR

1 μg of total RNA, 5 pmol of reverse primer and 20 U of SuperScript III reverse transcriptase (Life Technology) were mixed in 20 μl of RT buffer. To reverse transcribe the RNA, the reaction was incubated at 50 °C for 50 min. A tenth part of the RT reaction was used for cDNA amplification. The reaction was performed in 20 μl and contained 10 pmol of specific forward and reverse primers, 200 μM dNTPs, 1x Taq polymerase buffer and 1 U of Platinum Taq DNA polymerase (Life Technology). The amplification was carried out in an Eppendorf PCR System Thermocycler under the following conditions: initial denaturation for 30 s at 94 °C, 30 cycles of touchdown PCR with 30 s at 94 °C, 30 s at (65 °C–55 °C for first 20 cycles and 55 °C last 10 cycles) and an extension of 60 s at 72 °C. After the last cycle, the reaction was held for 5 min at the extension temperature to complete the amplification of all products. Primers used were: ACOXL-S2:GGCTCCAGATGGACAGTACC; ACOXL-AS2:AGG GTCTGTGTTTGGTGCTC; CGD91-F1 :GCTTGTGGCTGTGATAAGCA; CGD 91-R1:GCATTGTTCCTTTCCTGCAT; F-FIT2 :GAGAGCTACCTCAGCAACA AGC; R-FIT2 :GAGATGTCAAAGCCATGCCA; MAP2-F :CTGCACACTCACA TCCACCT; MAP2-R :TGTTCACCTTTCAGGACTGC; NR1H2-F :GGCTTCCAC TACAACGTGCT; NR1H2-R:TGACTGTGACTCCTGCTGCT; F-PEX11A :CG ACTCTTCAGAGCCACTCA; R-PEX11A:GCCTAGTCTGAACCATTTACGAC; PRKCE-F :AGCTGGCTGTCTTTCACGAT; PRKCE-R :CTGCAATGGGAGC AGTAGGT; ST3GAL2-F1 :AACCACCCACCATTTCATGT; ST3GAL2-R1 :TC CCAGTAGTGGTGCCAGTT; ST3GALNAC-F:GTGGCCTGTTCAATCTCTCC; ST3GALNAC-R:AGTCATGGGCATCGATGTTG; TUBB4-F :CAGTGACCTGCA ACTGGAGA; TUBB4-R:TCCTCGCGGATCTTACTGAT; CYPIIE1-F2 :CTG AAAGGGTGAAGGAGCAC; CYPIIE1-R2:GGTGATGAACCGCTGAATCT; TRAK2-F:ACAGACAGGGTGGAGCAGAT; TRAK2-R:GCTTTTTRAK2-FCTTG CAGCATTTCC.

2.5. Patient tissue

Tissue was received from the NICHD Brain and Tissue Bank that has received consent for the donation of tissue for research from the legal next of kin of all donors described. The Brain and Tissue Bank adheres to the standard of the Institutional Review Board of the University of Maryland School of Medicine in Baltimore, Maryland. Consents are on file in the office of the NICHD Brain and Tissue Bank.

2.6. Statistical analysis

For RT-PCR validation, changes in the gene expression were analyzed using unpaired t-tests (Graph Pad Prism 6 Software).

3. Results

3.1. Construction of SNORD116 and SNORD115 expression clones

To analyze the influence of *SNORD115* and *SNORD116* on gene expression, we generated a series of cDNA constructs. The SNORD expression cassette consists of two non-coding exons flanking an intron that hosts the snoRNA under the control of a CMV promoter (Fig. 1A, B).

We transfected HEK 293T cells with the *SNORD116* constructs and analyzed total RNA after 40 h of the transfection using RNase protection assay (RPA) (Fig. 1C). Endogenous *SNORD116* is not detectable using RPA in HEK 293T cells. Transfecting a cDNA expressing wild-type *SNORD116* results in detectable snoRNA expression that is however weaker than the expression observed in brain (Fig. 1D, E). We also overexpressed *SNORD115* using this approach, as previously described (Kishore and Stamm, 2006; Kishore et al., 2010) and found that HEK 293T cells do not express *SNORD115* endogenously (Fig. 1F, G).

To improve *SNORD116* expression, we thus mutated splice sites into the mammalian consensus. The 5′ splice site was mutated from TGgtaaggcac to **A**Ggtaag**tta**t and the 3′ splice site form gtgttgtcttcacag to **ctttc**tcttcacag. Improvement of the 5′ splice site strongly increased *SNORD116* expression, whereas changing the 3′ splice site had only a minor effect. Combining both splice site mutations showed no additional increase (Fig. 1D, E). Similar to previous reports (Shen et al., 2011), we observed shorter *SNORD116* fragments using these constructs that reflect the situation in brain. We thus used the *SNORD116* construct with the optimized 5′ splice site for further studies. The data show that *SNORD116* expression levels can be controlled at the level of splice site quality.

3.2. Array analysis of SNORD overexpression in HEK 293T cells

To determine the effect of SNORDs missing in PWS on gene expression, we performed four different array experiments using SpliceArrays (Affymetrix). Splicearrays are genomewide oligonucleotide-based arrays that are built on exon-specific probes (Johnson et al., 2003). Importantly, these arrays contain exon junction probes. Thus, in addition to a deregulation in overall gene expression, they detect changes in alternative splicing.

In the first three experiments, we transfected HEK 293T cell with constructs coding for (i) *SNORD115*, (ii) *SNORD116* and (iii) *SNORD115* and *SNORD116* together and compared them with overexpression of green fluorescent protein. The same amount of plasmid DNA was used in each experiment. The transfection of green fluorescent proteins controlled for equal amounts of promoter-containing plasmids transfected (Stoss et al., 1999). HEK 293T cells were used as they give high transfection efficiencies and express some neuronal markers (Lin et al., 2014). For each cell-based experiment three biological replicas were used. In the fourth experiment, we compared (iv) RNAs extracted from post-mortem posterior hypothalamus of PWS patients (two patients) and aged matched controls (three patients).

The overexpression of *SNORD115* and *SNORD116* was confirmed by RNase protection assay (Fig. 1D, F).

Overexpression of *SNORD115* resulted in 10 changes in gene expression (Supplemental Data 1, note that all supplemental data are hyperlinked to the UCSD genome browser). In addition, we observed nine changes in alternative splicing that however could not be validated by RT-PCR. Overexpression of *SNORD116* resulted in 274 changes in gene expression (Supplemental Data 2). For *SNORD116*, there were 47 changes in alternative cassette exon usage with low confidence that could not be validated by RT-PCR (data not shown). This suggests that the main effect of *SNORD116* is on expression levels of mRNAs, not their splicing patterns.

We next overexpressed *SNORD115* and *SNORD116* together to determine the simultaneous effect of the SNORDs as in most PWS patients both SNORDs are missing. In this experiment, we observed a total of 415 changes in gene expression (Supplemental Data 3). Changes in alternative splicing were minor, with only one change predicted with high confidence, which could not be validated by RT-PCR. Unexpectedly, changes in gene expression caused by simultaneous overexpression of *SNORD115* and *SNORD116* did only partially (23 genes) overlap with the changes in gene expression caused by *SNORD116* alone (Fig. 2). This suggests that *SNORD115* can modify the action of *SNORD116* on gene expression, suggesting that the major role for both snoRNAs is to work together to increase selected gene expression.

3.3. Array analysis of RNA isolated from PWS samples

We next compared the overall gene expression between PWS patients and aged matched controls in human posterior hypothalamus, the only currently available hypothalamic tissue. We choose hypothalamus, as dysfunctions in this brain region are the likely cause for most of the symptoms in PWS (Swaab, 1997). First, we confirmed the clinical diagnosis of PWS using RPA that confirmed the absence of *SNORD115* and *SNORD116* (Falaleeva et al., 2013). The comparison of PWS patient brains with aged match genetically normal controls showed 5113 changes in gene expression (Supplemental Data 4). The high number of differences in hypothalamic tissue likely reflects differences between individuals. However, we saw an overlap of 23 genes with the overexpression of *SNORD115/116* in HEK 293T cells (Fig. 2). A chi-squared test shows this overlap to be significant with a p-value of 7.35×10^{-3}. The direction of *SNORD115/116* induced changes was mostly similar, i.e. they were either downregulated in PWS and up-regulated through *SNORD115/116* overexpression, or up-regulated in PWS and downregulated in *SNORD115/116*

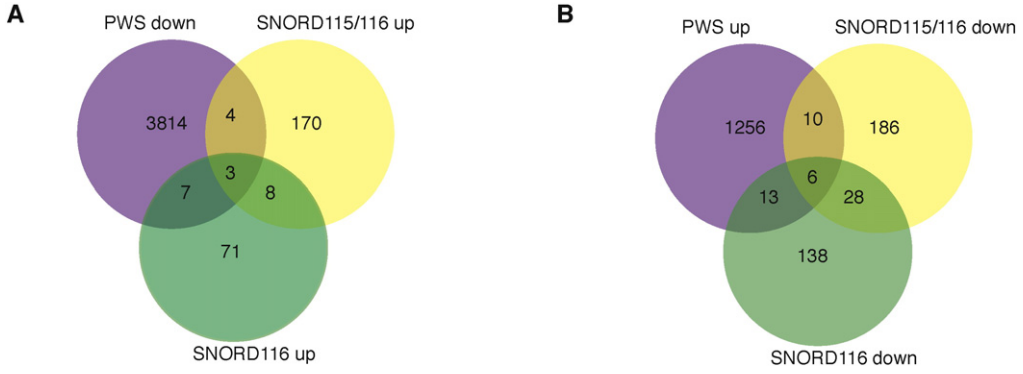

Fig. 2. Summary of array data. The Venn diagrams show the number of statistical significant changes in gene expression when SNORD115 and SNORD116 are overexpressed together, SNORD116 is overexpressed alone and when posterior hypothalamus from patients with PWS is compared with age-matched controls. A. The Venn diagram shows genes that are up-regulated by SNORD115/116 overexpression and are downregulated in PWS. B. The Venn diagram shows genes that are downregulated by SNORD115/116 overexpression and up-regulated in PWS. The gene names are listed in Supplemental data 5.

expression (Fig. 2A, B; Supplemental Data 5). In addition we detected several changes that showed different directions (Supplemental Data 5).

This suggested that some of these expression changes were directly caused by the loss of *SNORD115* and *SNORD116*. In summary, the loss of *SNORD116* and *SNORD115* expression in PWS caused mainly a deregulation in gene expression, not in alternative splicing.

3.4. Analysis of observed changes by RT-PCR

We next selected several regulated genes and validated observed changes by RT-PCR. To insure equal RNA loading, we measured *TRAK2* gene expression since *TRAK2* did not change in all array data sets (Supplemental Data 6). We found that changes in gene expression detected by the array resulted in changes determined by RT-PCR. However, for *NR1H2*, *ACOXL*, *PEX11A*, *ST3GAL2* genes there was a discrepancy in the direction of the change. It is possible that the probesets of the array do not fully reflect the complexity of the transcripts. Similar to the array experiments, the RT-PCR analysis revealed a synergistic action between the SNORDs, as *SNORD115* influenced the effect of *SNORD116* on gene expression (Table 1). A t-test analysis using three biological replicas showed that the effect of *SNORD115* on *SNORD116* action was statistically significant for *ST6GALNAC2*, *TUBB4*, *ACOXL* and *NR1H2* genes (Table 1). In all cases tested, the simultaneous expression of *SNORD115* and *SNORD116* increased expression of the target genes (Fig. 3). The genes up-regulated by *SNORD115/116* are always higher expressed in normal patients compared with PWS subjects, where the SNORDs are missing. Thus, *SNORD115/116* overexpression in cells reflects the situation in Prader–Willi patient samples.

In summary, the data indicate that *SNORD116* and *SNORD115* act synergistically to regulate the expression of several genes.

4. Discussion

4.1. SNORD115 and SNORD116 regulate gene expression levels

The Prader–Willi critical region contains two clusters of C/D box snoRNAs (SNORDs), *SNORD116* and *SNORD115*. The best understood function of C/D box snoRNAs is the guidance of RNA methylation activity to rRNA, using a defined part of this sequence, the antisense box. However, 137/267 human SNORDs have no sequence complementarity to known RNAs and are thus orphan (Dupuis-Sandoval et al., 2015).

SNORD115 shows an 18 nt sequence complementarity between its antisense box and the *serotonin receptor 2C* pre-mRNA. It was shown that *SNORD115* regulates alternative splicing of this receptor, which likely contributes to the hyperphagia in PWS (Kishore and Stamm, 2006). Subsequent analysis based on bioinformatic prediction showed that *SNORD115* regulates six other splicing events and importantly forms RNA–protein complexes that are different from the canonical snoRNPs. *SNORD115* forms shorter RNAs and associates with hnRNPs (Kishore et al., 2010; Soeno et al., 2010), suggesting the formation of a non-canonical complex. The serotonin receptor 2C is not expressed in HEK 293T cells and shows a very weak expression in posterior hypothalamus. We thus could not detect changes in serotonin receptor 2C expression. Similarly, the changes in alternative splicing previously detected by RT-PCR were too small to reach statistical significance in the array analysis.

SNORD116 has been considered to be of particular importance for PWS, as patients with microdeletions in *SNORD116* cluster show a phenotype related to PWS. The microdeletions have less severe phenotype than the full deletion of the PWS region (Cassidy et al., 2012). The molecular role of *SNORD116* is not clear, as bioinformatic analysis does not indicate strong sequence complementarity to any known RNA. However, *SNORD116* targets are predicted to be non-randomly associated with genes producing alternatively spliced mRNA isoforms (Bazeley et al., 2008).

To identify the effect of *SNORD116* on gene expression, we therefore overexpressed *SNORD116* in cells lacking endogenous *SNORD116* expression. We found changes in gene expression in 274 genes. It is possible that some of these changes are not direct. Unexpectedly, we could not find any changes in alternative splicing that could be validated by RT-PCR. Measured by both RT-PCR and array intensity, the changes caused by *SNORD116* are modest, less than twofold, similar to changes that were reported in a previous array experiment using lymphocytes from PWS subjects (Bittel et al., 2007).

Bioinformatic analysis did not reveal strong sequence complementarities between *SNORD116* sequences and their target genes. Recently, it was found that SNORDs can activate protein kinase R, a kinase that is activated by double-stranded RNAs, including those formed by SNORDs (Youssef et al., 2015). It remains to be determined whether *SNORD116* acts through such a mechanism, which will likely rely on limited sequence complementarity.

Almost all genes that we validated were up-regulated by *SNORD116/SNORD115*, suggesting that *SNORD115/116* in general promotes either stability or production of target mRNAs. We were not able to find long stretches of sequence complementarity in these regulated genes and thus the mechanism of action remains elusive.

It has been suggested that *SNORD115/SNORD116* containing regions form long ncRNA with snoRNA ends (Yin et al., 2012). Since we express only one copy of each SNORD, these long RNAs will not form and the effects we see were due to *SNORD116/SNORD115* acting on the level of

Table 1
Target gene validation. The percent change compared with GFP control is tabulated for each gene, i.e. the expression level after GFP transfection is set to 100% and the changes in gene expression after SNORD transfection expressed as a ratio (% change). The p-values were calculated using an unpaired two-tailed t-test from at least three different experiments. The TRAK2 gene was used as a control, as its expression did not change in multiple array experiments (this work and Zhang et al., 2013; Shen et al., 2013; Convertini et al., 2014).

Gene name	SNORD115 vs GFP		SNORD116 vs GFP		SNORD115 + 116 vs GFP		SNORD115 + 116 vs SNORD116		PWS vs control, brain	
	%change	p	%change	p	% change	p	Ratio	p	% change	p
ST6GALNAC2	62.05	0.0002	184.4	0.0035	122.3	0.0087	0.66	0.0125	44.5	0.0209
NR1H2	55.7	0.0736	80	0.0487	161.9	0.0486	2.02	0.0243	167	0.4513
ACOXL	89	0.2860	98.99	0.7939	140.4	0.0375	1.4	0.04	43.29	0.0432
TUBB4	219	0.0350	121.5	0.0001	167.9	0.0127	1.38	0.0429	41.22	0.0183
FIT2	99.06	0.9437	159.7	0.0003	197	0.0018	1.23	0.3097	32.98	0.0268
PEX11A	165	0.0252	162	0.0010	179	0.0005	1.1	0.1815	40	0.0123
MAP-2	133	0.0003	183	0.0039	169.2	0.0716	0.92	0.6862	28.5	0.0166
PRKCE	103.4	0.0760	125.8	0.0056	140.7	0.0087	1.12	0.2860	41.2	0.0146
ST3GAL2	103.8	0.0251	109.13	0.2266	118.2	0.5244	1.08	0.7528	58.7	0.0539
CGD91	90.7	0.0048	118.2	0.5360	122.5	0.3680	1.03	0.9075	11.7	0.0521
CYPIIE1	125.9	0.2168	107.25	0.7820	126.7	0.0296	1.18	0.4936	21.9	0.0282
TRAK2	98.13	0.4067	102.8	0.9110	95.3	0.1630	0.93	0.4305	112	0.2199

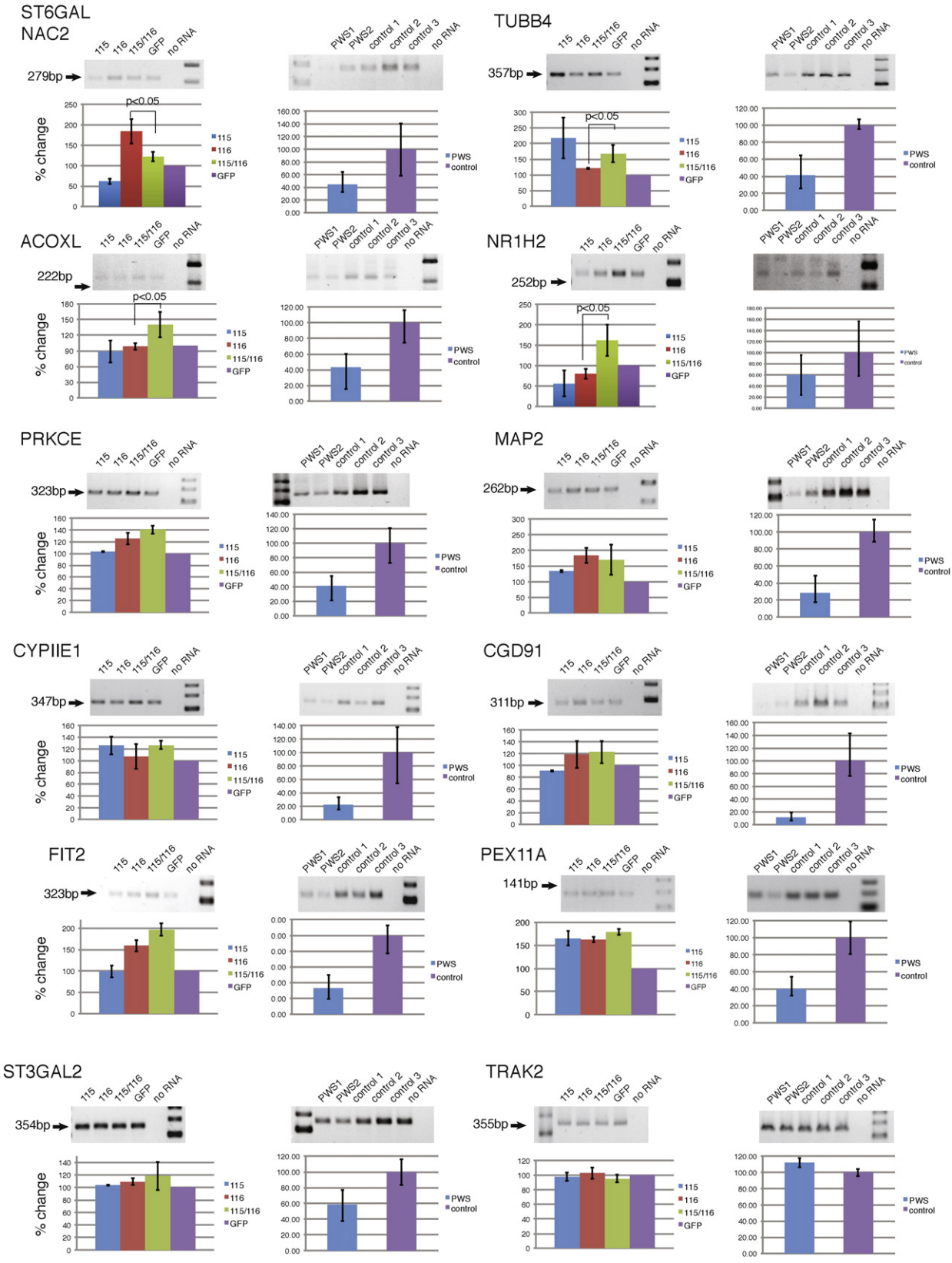

Fig. 3. Validation of array data. Selected changes in gene expression were validated using RT-PCR. The statistical analysis of at least three biological replicas for cells and two biological samples for PWS is shown underneath the gels. Error bars indicate the standard deviations. We used TRAK2 expression as a loading control since it shows no changes in all array experiments. The y-axis is the % change relative to the transfection of a GFP-expressing construct.

a short snoRNA. Similarly, our system will not detect changes caused by RNAs formed by the non-coding exons flanking the snoRNAs (Powell et al., 2013).

Some of the detected gene changes could be relevant for the observed phenotype. For example *ST6GALNAC2* is a sialyltransferases adding sialic acid to glycoproteins. One of its known interactors is

Mucin 1 (Marcos et al., 2011), a component of saliva. Thus a defect in mucin glycolsylation could contribute to changes in saliva seen in patients. Several genes identified (*ACOXL*, *CYPIIE1*, *FIT2*, *PEX11A*) are involved in lipid degradation/metabolism and their deregulation could contribute to changes in metabolism.

4.2. SNORD115 and SNORD116 modify each other's action on gene expression

To recapitulate the situation in PWS, we overexpressed *SNORD115* and *SNORD116* simultaneously and surprisingly found that *SNORD115* changes the number and intensity of genes regulated by *SNORD116*. This finding was confirmed by RT-PCR using ten selected genes. In most cases *SNORD115* enhances the increase of gene expression caused by *SNORD116* (Table 1, Fig. 3). Using t-test analysis we found that the influence of *SNORD115* on *SNORD116*-dependent genes is statistically significant for *ST6GALNAC2*, *TUBB4*, *ACOXL* and *NR1H2*. However, the molecular mechanism for the modulation of both SNORDs is unclear, because no extensive sequence complementarities can be detected between *SNORD116*, *SNORD115* and the four target genes. It is possible that *SNORD115* and *SNORD116* form heterodimers, which could be aided by binding proteins, as it is known that canonical C/D snoRNAs form dimers (Bleichert et al., 2009). The formation of heterodimers between *SNORD115* and *SNORD116*, possibly aided by proteins could explain why *SNORD115* modulates *SNORD116's* effects on gene expression.

The data could explain why a loss of *SNORD116* through microdeletions has a much milder phenotype than loss of both *SNORD115* and *SNORD116*. There are only two PWS-patients published that due to microdeletions do express *SNORD115* but not *SNORD116* (Fig. 1A). These patients are atypical, having a tall stature as a child, large head circumference, and lack of PWS facial gestalt and hand features atypical for PWS (Cassidy et al., 2012). Thus, both *SNORD115* and *SNORD116* contribute to the PWS disease etiology and should be considered for therapeutic development.

5. Conclusion

The two snoRNAs not expressed in Prader–Willi syndrome act together to regulate gene expression. *SNORD116* has the largest effect on the abundance of mRNAs. Therapies aimed for PWS should preferably target both *SNORD115* and *SNORD116* clusters.

Supplementary data to this article can be found online at http://dx.doi.org/10.1016/j.gene.2015.07.023. All genome coordinates in excel files are hyperlinked to the UCSC genome browser, allowing users to look up the respective genes. Of the 33,395 genes on the Affymetrix array, only 17,465 (52%) are annotated with a gene symbol to avoid ambiguities. Therefore some genes show no names but can be accessed through the hyperlink.

Acknowledgment

This work was supported by NIH01GM083187 (SS), R21R21HD080035 (SS); NIGMSP30GM110787, a grant from the Foundation for Prader-Willi Research, and a postdoctoral Fellowship 13POST16820024 from the American Heart Association (M.F.). This work utilized tissue from the NICHD Brain and Tissue Bank for Developmental Disorders (NICHD contract # HHSN275200900011C).

References

Bazeley, P.S., Shepelev, V., Talebizadeh, Z., Butler, M.G., Fedorova, L., Filatov, V., Fedorov, A., 2008. snoTARGET shows that human orphan snoRNA targets locate close to alternative splice junctions. Gene 408, 172–179.

Bieth, E., Eddiry, S., Gaston, V., Lorenzini, F., Buffet, A., Conte Auriol, F., Molinas, C., Cailley, D., Rooryck, C., Arveiler, B., Cavaille, J., Salles, J.P., Tauber, M., 2015. Highly restricted deletion of the SNORD116 region is implicated in Prader–Willi syndrome. Eur. J. Hum. Genet. 23, 252–255.

Bittel, D.C., Kibiryeva, N., Sell, S.M., Strong, T.V., Butler, M.G., 2007. Whole genome microarray analysis of gene expression in Prader–Willi syndrome. Am. J. Med. Genet. A 143, 430–442.

Bleichert, F., Gagnon, K.T., Brown 2nd, B.A., Maxwell, E.S., Leschziner, A.E., Unger, V.M., Baserga, S.J., 2009. A dimeric structure for archaeal box C/D small ribonucleoproteins. Science 325, 1384–1387.

Bortolin-Cavaille, M.L., Cavaille, J., 2012. The SNORD115 (H/MBII-52) and SNORD116 (H/MBII-85) gene clusters at the imprinted Prader–Willi locus generate canonical box C/D snoRNAs. Nucleic Acids Res. 40, 6800–6807.

Brown, J.W., Marshall, D.F., Echeverria, M., 2008. Intronic noncoding RNAs and splicing. Trends Plant Sci. 13, 335–342.

Butler, M.G., 2011. Prader–Willi syndrome: obesity due to genomic imprinting. Curr. Genet. 12, 204–215.

Butler, M.G., Hanchett, J.M., Thompson, T.E., 2006. Clinical findings and natural history of Prader–Willi syndrome. In: Butler, M.G., Lee, P.D.K., Whitman, B.Y. (Eds.), Management of Prader–Willi Syndrome. Springer, pp. 3–48.

Cassidy, S.B., Schwartz, S., Miller, J.L., Driscoll, D.J., 2012. Prader–Willi syndrome. Genet. Med. 14, 10–26.

Convertini, P., Shen, M., Potter, P.M., Palacidos, G., Lagisetti, C., de la Grange, P., Horinski, C., Mittendorf, Y., Webb, T.R., Stamm, S., 2014. Sudemycin E influences alternative splicing and changes chromatin modifications. Nucleic Acids Res. 4947–4961.

de Smith, A.J., Purmann, C., Walters, R.G., Ellis, R.J., Holder, S.E., Van Haelst, M.M., Brady, A.F., Fairbrother, U.L., Dattani, M., Keogh, J.M., Henning, E., Yeo, G.S., O'Rahilly, S., Froguel, P., Farooqi, I.S., Blakemore, A.I., 2009. A deletion of the HBII-85 class of small nucleolar RNAs (snoRNAs) is associated with hyperphagia, obesity and hypogonadism. Hum. Mol. Genet. 18, 3257–3265.

Deschamps-Francoeur, G., Garneau, D., Dupuis-Sandoval, F., Roy, A., Frappier, M., Catala, M., Couture, S., Barbe-Marcoux, M., Abou-Elela, S., Scott, M.S., 2014. Identification of discrete classes of small nucleolar RNA featuring different ends and RNA binding protein dependency. Nucleic Acids Res. 42, 10073–10085.

Duker, A.L., Ballif, B.C., Bawle, E.V., Person, R.E., Mahadevan, S., Alliman, S., Thompson, R., Traylor, R., Bejjani, B.A., Shaffer, L.G., Rosenfeld, J.A., Lamb, A.N., Sahoo, T., 2010. Paternally inherited microdeletion at 15q11.2 confirms a significant role for the SNORD116 C/D box snoRNA cluster in Prader–Willi syndrome. Eur. J. Hum. Genet. 18, 1196–1201.

Dupuis-Sandoval, F., Poirier, M., Scott, M.S., 2015. The emerging landscape of small nucleolar RNAs in cell biology. Wiley Interdiscip. Rev. RNA 6, 381–397.

Falaleeva, M., Stamm, S., 2013. Processing of snoRNAs as a new source of regulatory noncoding RNAs: snoRNA fragments form a new class of functional RNAs. Bioessays 35, 46–54.

Falaleeva, M., Sulsona, C.R., Zielke, H.R., Currey, K.M., de la Grange, P., Aslanzadeh, V., Driscoll, D.J., Stamm, S., 2013. Molecular characterization of a patient presumed to have Prader–Willi syndrome. Clinical Medicine Insights. Case Reports 6 pp. 79–86.

Hirose, T., Steitz, J.A., 2001. Position within the host intron is critical for efficient processing of box C/D snoRNAs in mammalian cells. Proc. Natl. Acad. Sci. U. S. A. 98, 12914–12919.

Johnson, J.M., Castle, J., Garrett-Engele, P., Kan, Z., Loerch, P.M., Armour, C.D., Santos, R., Schadt, E.E., Stoughton, R., Shoemaker, D.D., 2003. Genome-wide survey of human alternative pre-mRNA splicing with exon junction microarrays. Science 302, 2141–2144.

Kapur, K., Jiang, H., Xing, Y., Wong, W.H., 2008. Cross-hybridization modeling on Affymetrix exon arrays. Bioinformatics 24, 2887–2893.

Kishore, S., Stamm, S., 2006. The snoRNA HBII-52 regulates alternative splicing of the serotonin receptor 2C. Science 311, 230–232.

Kishore, S., Khanna, A., Zhang, Z., Hui, J., Balwierz, P.J., Stefan, M., Beach, C., Nicholls, R.D., Zavolan, M., Stamm, S., 2010. The snoRNA MBII-52 (SNORD 115) is processed into smaller RNAs and regulates alternative splicing. Hum. Mol. Genet. 19, 1153–1164.

Kiss, T., 2002. Small nucleolar RNAs: an abundant group of noncoding RNAs with diverse cellular functions. Cell 109, 145–148.

Lestrade, L., Weber, M.J., 2006. snoRNA-LBME-db, a comprehensive database of human H/ACA and C/D box snoRNAs. Nucleic Acids Res. 34, D158-62.

Lin, Y.C., Boone, M., Meuris, L., Lemmens, I., Van Roy, N., Soete, A., Reumers, J., Moisse, M., Plaisance, S., Drmanac, R., Chen, J., Speleman, F., Lambrechts, D., Van de Peer, Y., Tavernier, J., Callewaert, N., 2014. Genome dynamics of the human embryonic kidney 293 lineage in response to cell biology manipulations. Nat. Commun. 5, 4767.

Marcos, N.T., Bennett, E.P., Gomes, J., Magalhaes, A., Gomes, C., David, L., Dar, I., Jeanneau, C., DeFrees, S., Krustrup, D., Vogel, L.K., Kure, E.H., Burchell, J., Taylor-Papadimitriou, J., Clausen, H., Mandel, U., Reis, C.A., 2011. ST6GalNAc-I controls expression of sialyl-Tn antigen in gastrointestinal tissues. Front. Biosci. 3, 1443–1455.

Matera, A.G., Terns, R.M., Terns, M.P., 2007. Non-coding RNAs: lessons from the small nuclear and small nucleolar RNAs. Nat. Rev. Mol. Cell Biol. 8, 209–220.

Powell, W.T., Coulson, R.L., Crary, F.K., Wong, S.S., Ach, R.A., Tsang, P., Alice Yamada, N., Yasui, D.H., Lasalle, J.M., 2013. A Prader–Willi locus lncRNA cloud modulates diurnal genes and energy expenditure. Hum. Mol. Genet. 22, 4318–4328.

Reichow, S.L., Hamma, T., Ferre-D'Amare, A.R., Varani, G., 2007. The structure and function of small nucleolar ribonucleoproteins. Nucleic Acids Res. 35, 1452–1464.

Sahoo, T., del Gaudio, D., German, J.R., Shinawi, M., Peters, S.U., Person, R.E., Garnica, A., Cheung, S.W., Beaudet, A.L., 2008. Prader–Willi phenotype caused by paternal deficiency for the HBII-85 C/D box small nucleolar RNA cluster. Nat. Genet. 40, 719–721.

Shen, S., Warzecha, C.C., Carstens, R.P., Xing, Y., 2010. MADS+: discovery of differential splicing events from Affymetrix exon junction array data. Bioinformatics 26, 268–269.

Shen, M., Eyras, E., Wu, J., Khanna, A., Josiah, S., Rederstorff, M., Zhang, M.Q., Stamm, S., 2011. Direct cloning of double-stranded RNAs from RNase protection analysis reveals processing patterns of C/D box snoRNAs and provides evidence for widespread antisense transcript expression. Nucleic Acids Res. 39, 9720–9730.

Shen, M., Bellaousov, S., Hiller, M., de La Grange, P., Creamer, T.P., Malina, O., Sperling, R., Mathews, D.H., Stoilov, P., Stamm, S., 2013. Pyrvinium pamoate changes alternative splicing of the serotonin receptor 2C by influencing its RNA structure. Nucleic Acids Res. 41, 3819–3832.

Smith, C.M., Steitz, J.A., 1997. Sno storm in the nucleolus: new roles for myriad small RNPs. Cell 89, 669–672.

Soeno, Y., Taya, Y., Stasyk, T., Huber, L.A., Aoba, T., Huttenhofer, A., 2010. Identification of novel ribonucleo–protein complexes from the brain-specific snoRNA MBII-52. RNA 16, 1293–1300.

Stoss, O., Stoilov, P., Hartmann, A.M., Nayler, O., Stamm, S., 1999. The in vivo minigene approach to analyze tissue-specific splicing. Brain Res. Protocol. 4, 383–394.

Swaab, D.F., 1997. Prader–Willi syndrome and the hypothalamus. Acta Paediatr. Suppl. 423, 50–54.

Yin, Q.F., Yang, L., Zhang, Y., Xiang, J.F., Wu, Y.W., Carmichael, G.G., Chen, L.L., 2012. Long noncoding RNAs with snoRNA ends. Mol. Cell 48, 219–230.

Youssef, O.A., Safran, S.A., Nakamura, T., Nix, D.A., Hotamisligil, G.S., Bass, B.L., 2015. Potential role for snoRNAs in PKR activation during metabolic stress. Proc. Natl. Acad. Sci. U. S. A. 112, 5023–5028.

Zhang, Z., Convertini, P., Shen, M., Xu, X., Lemoine, F., de la Grange, P., Andres, D.A., Stamm, S., 2013. Valproic acid causes proteasomal degradation of DICER and influences miRNA expression. PLoS ONE 8, e82895.